

## Dehydrochlorination of Poly(vinyl chloride) Modified with Titanium Dioxide/Poly(ethylene oxide) Based Paint Photocatalysts

Kensuke Miyazaki, Hiroaki Sato, Shinpei Kikuchi, Hisayuki Nakatani

Department of Biotechnology and Environmental Chemistry, Kitami Institute of Technology,  
165 Koen-Cho, Kitami, Hokkaido 090-8507, Japan  
Correspondence to: H. Nakatani (E-mail: nakatani@chem.kitami-it.ac.jp)

**ABSTRACT:** The dehydrochlorination of poly(vinyl chloride) (PVC) film samples modified with titanium dioxide (TiO<sub>2</sub>)/poly(ethylene oxide) (PEO) based paint photocatalysts [the addition of methyl linoleate (ML) or methyl oleate (MO)] was performed. After 24 h of UV photoirradiation, the sample with TiO<sub>2</sub>/PEO showed that there existed a structure with the longest polyene length, whereas that with TiO<sub>2</sub>/PEO/ML contained the most polyene structures. The chloroform-soluble fraction of the sample with TiO<sub>2</sub>/PEO contained a poly(vinyl alcohol) (PVA) structure instead of a polyene one and showed a novel method of PVA production via PVC photodegradation. The molecular weight curve of the fraction shifted slightly to a lower molecular weight compared to that without the photocatalyst; this showed that slight polymer chain scission occurred. The <sup>1</sup>H-NMR and <sup>13</sup>C-NMR spectra showed that the content of PVA units was about 20%, and the PVA sequence was blocky. The fraction of the sample with TiO<sub>2</sub>/PEO/ML contained the highest methyl group content; this showed that the branch degree was highest as was the polyene content. These highest contents were due to the existence of the grafted ML. Pyrolysis gas chromatography/mass spectroscopy measurements suggested that there existed more polyene and graft units in the chloroform-insoluble fractions of the samples with TiO<sub>2</sub>/PEO, TiO<sub>2</sub>/PEO/ML, and TiO<sub>2</sub>/PEO/MO, respectively. © 2014 Wiley Periodicals, Inc. *J. Appl. Polym. Sci.* **2014**, *131*, 40760.

**KEYWORDS:** degradation; irradiation; poly(vinyl chloride); recycling

Received 4 December 2013; accepted 24 March 2014

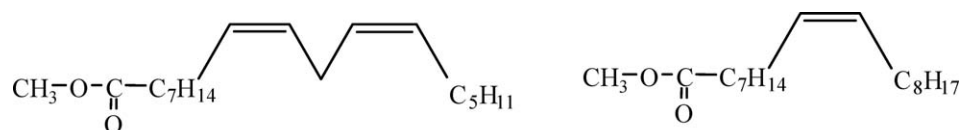
DOI: 10.1002/app.40760

### INTRODUCTION

Poly(vinyl chloride) (PVC) is a common polymeric material and is widely used as an industrial one. Although PVC has many attractive properties, its waste is not good for the environment because of its chlorine content.<sup>1</sup> Many investigators have proposed recycling methods based on the evaluated temperature to prevent the formation of toxic chloride compounds.<sup>1–5</sup> In particular, the production of substitutions for PVC, such as poly(vinyl alcohol) (PVA), has attracted much attention from the viewpoint of upgraded recycling.<sup>1,2,5</sup> Such PVA production with a photochemical reaction would show good productivity because an expensive heating unit and/or heat-resistant container are not used. However, the application of the photochemical reaction has been hardly performed. PVC dehydrochlorination is readily caused by photoirradiation, and this leads to the formation of a polyacetylene-like polymer composed of a polyene structure.<sup>2,6</sup> The solubility of polyacetylene for various solvents is poor as is its processability. Therefore, the application of a substituted PVC has been difficult.

If PVA is produced via a simple PVC photochemical reaction, such as photodegradation, its application has a high degree of availability as a novel PVC recycler.

In our previous work,<sup>7,8</sup> we succeeded in photodegrading polystyrene (PS) and polypropylene (PP) films with titanium dioxide (TiO<sub>2</sub>)/poly(ethylene oxide) (PEO) and TiO<sub>2</sub>/PEO/methyl linoleate (ML) paint photocatalysts. Polymer photodegradation with TiO<sub>2</sub> photocatalysis has been studied.<sup>9–12</sup> TiO<sub>2</sub> is photoexcited and produces an electron and positive hole. The electron and positive hole react with H<sub>2</sub>O and O<sub>2</sub> and then form OH radical species.<sup>13,14</sup> The radical species has a high reactive ability and initiates polymer degradation.<sup>10,13</sup> The degradation rate is, however, considerably slower because of the nonexistence of H<sub>2</sub>O in the polymeric matrix. To improve the PP degradation rate, we added PEO to the TiO<sub>2</sub> photocatalyst.<sup>15,16</sup> PEO was hydrophilic and could adsorb moisture in the atmosphere. TiO<sub>2</sub> reacted with an adsorbed H<sub>2</sub>O in the PEO phase and produced OH radical species. The reaction of the PEO and radical species produced acid and aldehyde compounds, and this brought



Methyl linoleate (ML)

Methyl oleate (MO)

Figure 1. Chemical structures of ML and MO.

about the facilitation of the PP degradation.<sup>17,18</sup> In addition, H<sub>2</sub>O was reproduced, and then, these reactions were repeated until the PEO component was completely consumed. The higher PP photodegradation rate was due to the coexistence of the TiO<sub>2</sub> and PEO components.<sup>15,16</sup> Moreover, the additional ML component certainly blocked a PS crosslinking reaction and PP chemi-crystallization and accelerated their photodegradation rate.

In this study, the dehydrochlorination of a PVC film sample was performed with three kinds of paint photocatalysts [TiO<sub>2</sub>/PEO, TiO<sub>2</sub>/PEO/ML, and TiO<sub>2</sub>/PEO/methyl oleate (MO)]. After these photocatalysts was painted on the samples, they were photoirradiated by UV light. The polyene structures that we obtained were analyzed with an ultraviolet–visible (UV–vis) spectrophotometer. The phototreated samples were fractionated with boiling chloroform. The soluble fractions were analyzed with gel permeation chromatography (GPC) and NMR spectroscopy, respectively. On the other hand, the insoluble fractions were analyzed with pyrolysis gas chromatography/mass spectroscopy (Py-GC/MS) spectroscopy.

We studied the modification of the PVC dehydrochlorination process with the paint photocatalysts and succeeded in developing a novel synthetic process of PVA.

## EXPERIMENTAL

### Materials

PVC was purchased from Sigma-Aldrich Co., LLC. The number-average molecular weight and polydispersity (weight-average molecular weight/number-average molecular weight) were  $4.7 \times 10^4$  and 1.7, respectively. PEO was purchased from Wako Pure Chemical Industries, Ltd. The average molecular weight was  $5.0 \times 10^5$ . TiO<sub>2</sub> (anatase-type, diameter  $\approx 5 \mu\text{m}$ ), ML and MO were purchased from Wako Pure Chemical Industries. The purities of the ML and MO were greater than 98 and 99%, respectively. Figure 1 shows the chemical structures of ML and MO.

### Preparation of PVC Film

The PVC pellets were molded into a film ( $30 \times 30 \times 0.2 \text{ mm}^2$ ) by compression molding at 160°C under 10 MPa for 5 min and successively under 50 MPa for 5 min.

### Painting of the Photocatalyst on the PVC Film

The paint conditions on the PVC film were as follows: (1) a 50-mL water solution containing 10 mg of TiO<sub>2</sub> and 500 mg of PEO was prepared (TiO<sub>2</sub>/PEO), (2) a 25-mL water solution containing 5 mg of TiO<sub>2</sub> and 250 mg of PEO + 25 mL of ML was prepared (TiO<sub>2</sub>/PEO/ML), and (3) a 25-mL water solution containing 5 mg of TiO<sub>2</sub> and 250 mg of PEO and 25 mL of MO was prepared (TiO<sub>2</sub>/PEO/MO). These solutions were painted on the film surface and were dried at room temperature

to remove the water component. The paint amounts were 10 g of solution/g of film for a 0.2 mm thick film with the same surface ( $30 \times 30 \text{ mm}^2$ ).

### Photoirradiation Conditions

The  $30 \times 30 \text{ mm}^2$  film was laid on a Petri dish. A 400-W mercury vapor lamp (Toshiba H-400P, luminance value = 200 cd/cm<sup>2</sup>) was used as a UV light source. The distance between the specimens and the lamp was 50 cm. The photoirradiation was carried out at 30°C for 24 h. With our previous results,<sup>7</sup> the performance of the photocatalyst could be not maintained for more time. All of the photoirradiated films were washed with methanol solvent and dried before the measurements.

### UV–Vis Spectrophotometer Analysis

The UV–vis spectra of 16 scans were recorded on a Shimadzu Multi Spec-1500.

### Boiling Chloroform Extraction

The chloroform extraction was performed with a Soxhlet extraction apparatus. Approximately 1.2 g of the photoirradiated sample was cut into  $30 \times 5\text{-mm}^2$  rectangles and was placed in a  $24 \times 100 \text{ mm}^2$  extraction thimble (Advantec 86R, Toyo Roshi Kaisha, Ltd.). It was extracted with 100 mL of chloroform for 7 h in a Soxhlet apparatus. After the extraction, the soluble part was thoroughly dried with a rotary evaporator at room temperature, and its weight was measured. The chloroform-soluble ratio was defined as follows:

$$\begin{aligned} & \text{Chloroform-soluble ratio (wt \%)} \\ & = \text{Soluble part weight / Sample weight} \times 100 \end{aligned}$$

The chloroform-soluble part obtained was analyzed with GPC and <sup>1</sup>H-NMR measurements, and the insoluble part was obtained with a Py-GC/MS one.

### GPC Analysis

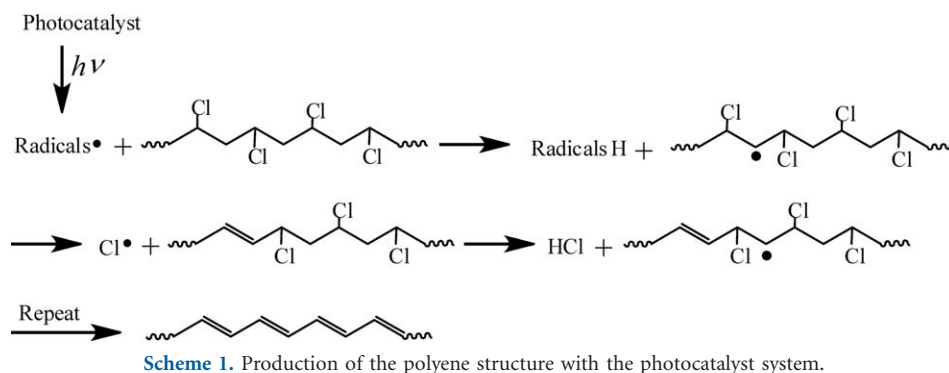
A sample in a small vial was dissolved in 5 mL of chloroform, and the obtained sample solution was directly measured by GPC. The molecular weight was determined by GPC (Shimadzu, Prominence GPC system with a GPC-80MC column, Shimadzu Co., Japan) at 40°C with chloroform as a solvent and was calibrated with PS standards.

### NMR Spectroscopy Measurement

The NMR spectrum was measured with a JEOL EX-400 spectrometer at 20°C in chloroform-*d*. Tetramethylsilane was added as an internal chemical shift reference.

### Py-GC/MS Measurement

A furnace-type pyrolyzer was applied in this study. It had a vertical microfurnace and temperature-programming capability. The multifunctional pyrolyzer (Frontier Labs, EGA/PY-3030D)



was attached to a gas chromatography (GC)/mass spectroscopy (MS) instrument (Shimadzu, GCMS-QP2010 PLUS). The measurement was done with the chloroform insoluble fraction (500  $\mu\text{g}$ ). The fraction sample was heated at a rate of 30°C/min from 100 to 200°C and was then kept for 3 min to remove the solvent. The fast pyrolysis was performed at 350, 450, and 550°C. The GC/MS ion source and interface were kept at 200 and 300°C, respectively. Helium was used as the carrier gas for the capillary column with a flow rate of 1.0 mL/min. The MS system was operated under electron ionization mode at 70 eV and in a scan range of mass-to-charge ratio ( $m/z$ ) of 10–300.

## RESULTS AND DISCUSSION

PVC dehydrochlorination was induced by photoirradiation; as a result, a polyene structure was produced. As shown in Scheme 1, the photocatalyst generated radical species and facilitated the dehydrochlorination. Figure 2 shows the UV–vis spectra of the pristine PVC and 24-h-photoirradiated PVC samples with various photocatalysts. It is known that the maximum absorption moves to a longer wavelength with increasing polyene length.<sup>19</sup> The order of the 24-h-photoirradiated PVC samples showed a longer wavelength at the maximum absorbance as follows: With  $\text{TiO}_2/\text{PEO}$  > With  $\text{TiO}_2/\text{PEO}/\text{ML}$   $\geq$  Without photocatalyst > Pristine > With  $\text{TiO}_2/\text{PEO}/\text{MO}$ . On the other hand, the order of the absorbance intensity was as follows: With  $\text{TiO}_2/\text{PEO}/\text{ML}$  >  $\text{TiO}_2/\text{PEO}$  = Without photocatalyst > Pristine > With

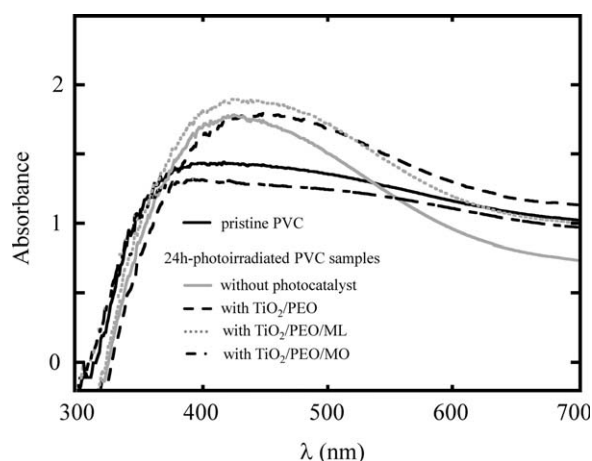


**Figure 2.** UV–vis spectra of the pristine PVC and 24-h-photoirradiated PVC samples with various photocatalysts.

$\text{TiO}_2/\text{PEO}/\text{MO}$ . The intensity was correlated with the amount of polyene units; this showed that the sample with  $\text{TiO}_2/\text{PEO}/\text{ML}$  had the greatest amount of the unit among these samples. Although the sample with  $\text{TiO}_2/\text{PEO}$  had the longest polyene length, the amount of polyene was lower than that with  $\text{TiO}_2/\text{PEO}/\text{ML}$ . These results suggest that there was a difference in the reactions induced by these photocatalysts. After dehydrochlorination, radical addition reactions were successively caused by the photocatalysts. It seemed that the frequency in the radical addition reaction and the kind of added functional group depended on the kinds of photocatalyst.

Figure 3 shows the chloroform-soluble fractions of the pristine PVC and 24-h-photoirradiated PVC samples with various photocatalysts. The pristine PVC was heat-treated during compression molding, and the chain branching, including crosslinking, was certainly caused. Therefore, there existed about an 80% insoluble fraction in the PVC. The order of the soluble fraction amount was as follows: Pristine (18.6%) > With  $\text{TiO}_2/\text{PEO}$  (13.2%) > With  $\text{TiO}_2/\text{PEO}/\text{ML}$  (7.9%)  $\geq$  Without photocatalyst (7.0%) > With  $\text{TiO}_2/\text{PEO}/\text{MO}$  (3.3%). Among the 24-h-photoirradiated PVC samples, the sample with  $\text{TiO}_2/\text{PEO}$  provided the largest soluble fraction. The amount of the soluble fraction with  $\text{TiO}_2/\text{PEO}/\text{ML}$  was about 60% of that with  $\text{TiO}_2/\text{PEO}$ . The amount of the soluble fraction with  $\text{TiO}_2/\text{PEO}/\text{MO}$  was the lowest. The MO chemical structure was similar to that of ML, and the difference was only the number of carbon–carbon double bonds (see Figure 1). On the other hand, the

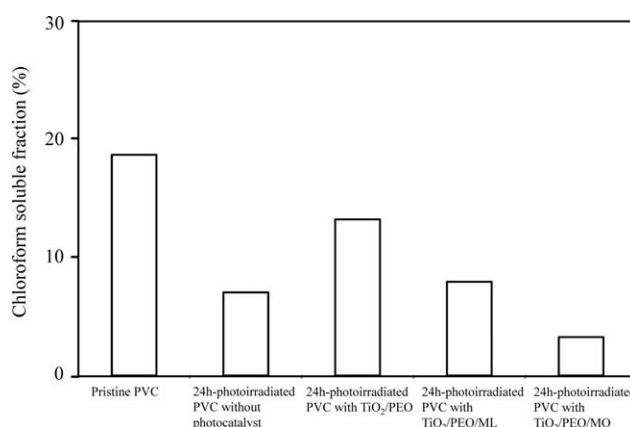


**Figure 3.** Chloroform-soluble fractions of the pristine PVC and 24-h-photoirradiated PVC samples with various photocatalysts.

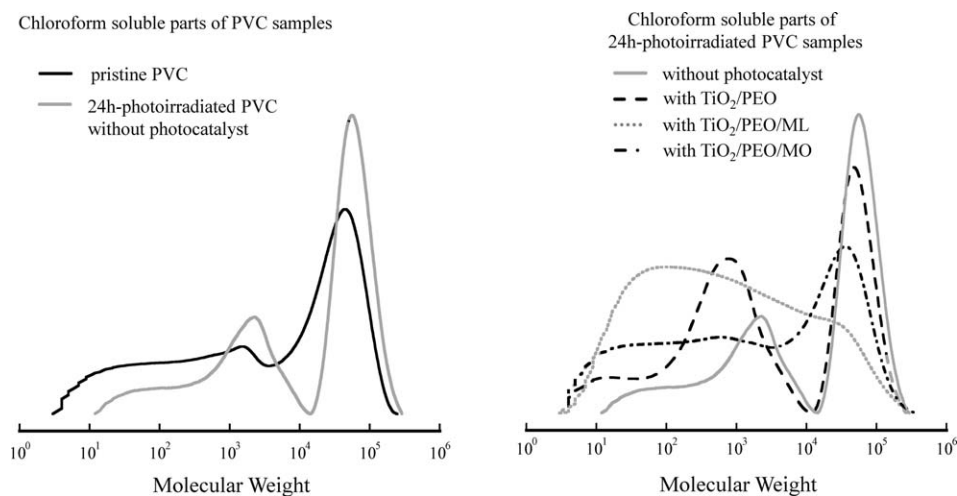


**Figure 4.** Differential molecular weight distribution curves of the chloroform-soluble parts of the pristine PVC and 24-h-photoirradiated PVC samples with various photocatalysts.

amount of the soluble fraction with  $\text{TiO}_2/\text{PEO}/\text{MO}$  was only 50% of that with  $\text{TiO}_2/\text{PEO}/\text{ML}$ , and the additive effect on the PVC solubilization was considerably less. Figure 4 shows the differential molecular weight distribution curves of the chloroform-soluble fractions. The curve of the 24-h-photoirradiated PVC without photocatalyst shifted to a higher molecular weight compared with that of the pristine one. This behavior was due to the crosslinking reaction. The curves of the samples with  $\text{TiO}_2/\text{PEO}$ ,  $\text{TiO}_2/\text{PEO}/\text{ML}$  and  $\text{TiO}_2/\text{PEO}/\text{MO}$  showed different behavior, respectively. The curve of PVC with  $\text{TiO}_2/\text{PEO}$  shifted slightly to a lower molecular weight compared to that without photocatalyst, and the peak in the low-molecular-weight region was developed. It seemed that a slight polymer chain scission occurred. The curve shape of the PVC with  $\text{TiO}_2/\text{PEO}/\text{ML}$  became much broader compared to those without photocatalyst and with  $\text{TiO}_2/\text{PEO}$ . The molecular weight drastically decreased, and this suggested that vigorous chain scission occurred. On the other hand, the curve of the PVC with  $\text{TiO}_2/\text{PEO}/\text{MO}$  was located between those without photocatalyst and with  $\text{TiO}_2/\text{PEO}/\text{ML}$  and its shape had both of their characteristics. Figure 5 shows the low-molecular-weight

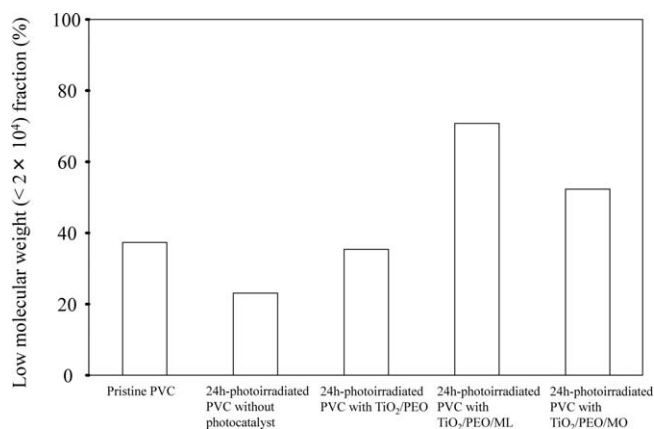


**Figure 5.** Low-molecular-weight ( $< 2 \times 10^4$ ) fraction (%) of the pristine PVC and 24-h-photoirradiated PVC samples with various photocatalysts.

( $< 2 \times 10^4$ ) fractions. The fraction of the 24-h-photoirradiated PVC with  $\text{TiO}_2/\text{PEO}/\text{ML}$  was approximately two times higher than that of the pristine one. In our previous work,<sup>7</sup> we succeeded in photodegrading a PS film with a  $\text{TiO}_2/\text{PEO}/\text{ML}$  paint photocatalyst system. The additional ML component certainly blocked a PS crosslinking reaction and accelerated the photodegradation rate. The ML worked as antiblocking agent for PVC as well. ML had allyl hydrogens and became a stable radical because of its radical resonance structure. Therefore, ML was suitable as source of such small radical molecules for graft polymerization with the unsaturated and/or radical PVC molecules. When the photoirradiation to the PVC samples was performed, a competition reaction between the PVC chain scission and crosslinking was certainly caused. The ML certainly blocked the crosslinking reaction; this led to a decreasing molecular weight. MO had the same ability because of its chemical structure. However, its grafting efficiency was considerably lower. The radical stability of MO was less than that of ML because MO had only one unsaturated group (carbon-carbon double bond) in the chemical structure (see Figure 1). The lower radical stability led to fewer blocking crosslinking reactions.

The chloroform-soluble fractions were characterized by  $^1\text{H-NMR}$  measurement. The obtained internal double-bond and

**Table I.** Contents of Internal Double Bonds and Methyl Groups in Chloroform-Soluble Fractions of Various PVC Samples

Chloroform-soluble fraction	Internal double bond/1000 VC	Methyl group/1000 VC
Pristine PVC	0.8	6.3
24-h-Photoirradiated PVC samples		
Without photocatalyst	1.4	11.9
With $\text{TiO}_2/\text{PEO}$	0.1	0.3
With $\text{TiO}_2/\text{PEO}/\text{ML}$	1.6	17.2
With $\text{TiO}_2/\text{PEO}/\text{MO}$	0.3	4.1

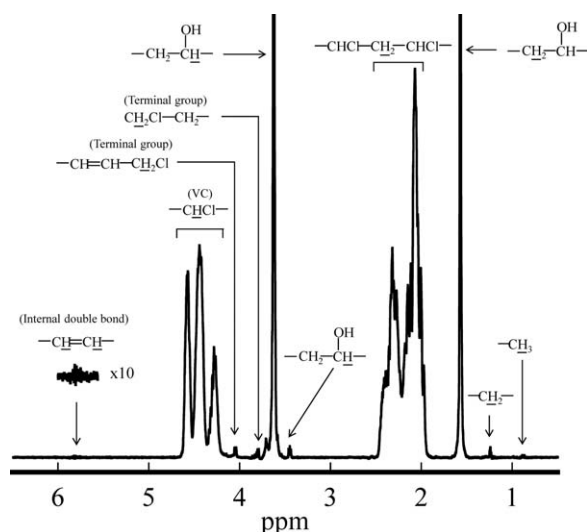


**Figure 6.**  $^1\text{H-NMR}$  spectrum of the chloroform-soluble fraction of the 24-h-photoirradiated PVC with  $\text{TiO}_2/\text{PEO}$ .

methyl group contents (per 1000 VC =  $-\text{CHCl}-$  units) are summarized in Table I. The methyl group content provided an indication of the branching degree. The soluble fraction of the sample with  $\text{TiO}_2/\text{PEO}$  showed the minimum values among these samples. Figure 6 shows the  $^1\text{H-NMR}$  spectrum of the chloroform-soluble fraction of the sample with  $\text{TiO}_2/\text{PEO}$ . The apparent resonances assigned to the PVA unit appeared around 1.6, 3.5, and 3.6 ppm, respectively. The content of the PVA unit was estimated from the ratio of the PVA peak area at 1.6 to the PVC one around 2.3 ppm and was approximately 20%.

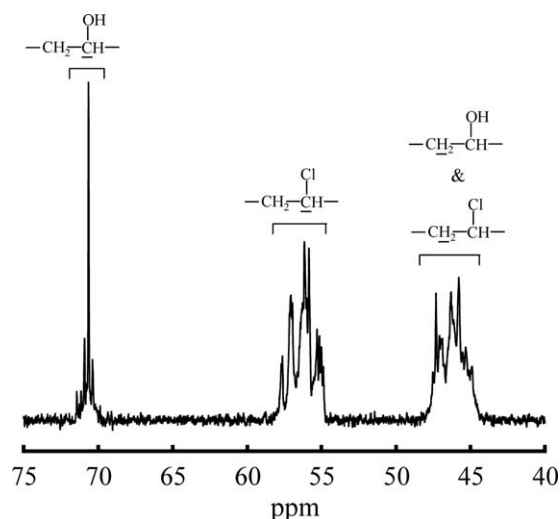
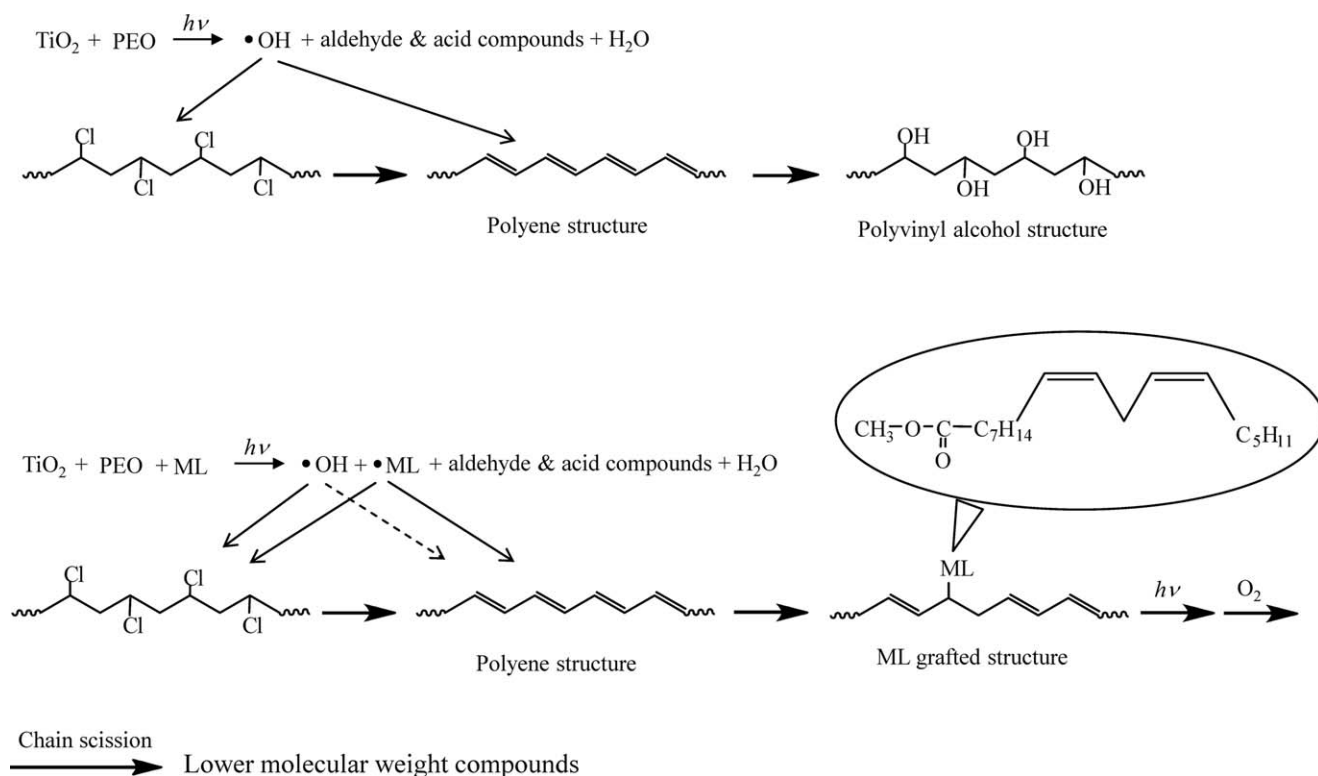


**Figure 7.**  $^{13}\text{C-NMR}$  spectrum of the chloroform-soluble fraction of the 24-h-photoirradiated PVC with  $\text{TiO}_2/\text{PEO}$ .

As shown in Scheme 2, the internal double bond reacted with the OH radical species generated by the photocatalytic PEO photodegradation with  $\text{TiO}_2$ . PVC dehydrochlorination produced a polyene compound, that is, a polyacetylene-like polymer.<sup>2,6</sup> Figure 7 shows the  $^{13}\text{C-NMR}$  spectrum. The methine carbon resonances assigned to PVA and PVC appeared around 71 and 56 ppm, respectively. Each of the resonances split into multiplets, and this indicated that there existed stereochemical sequence distributions (i.e., tacticity) in the corresponding methine carbons. These multiresonances reflected a specific



**Scheme 2.** Schematic reaction paths of PVA and lower molecular weight compounds produced with the  $\text{TiO}_2/\text{PEO}$  and  $\text{TiO}_2/\text{PEO}/\text{ML}$  photocatalysts.

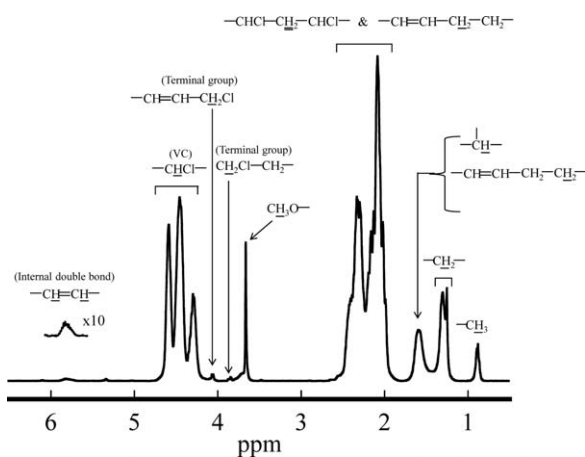


**Figure 8.**  $^1\text{H}$ -NMR spectrum of the chloroform-soluble fraction of the 24-h-photoirradiated PVC with  $\text{TiO}_2/\text{PEO}/\text{ML}$ .

reaction mechanism of the OH substitution. The carbon-carbon double bond was continuously produced by dehydrochlorination<sup>20</sup> and then selectively reacted with the OH radical species, as shown in Scheme 2. Accordingly, a blocky PVA sequence was produced. The OH multiresonance demonstrated that the OH substitution proceeded by a two-step reaction. The processability of the polyacetylene-like polymer was too poor to have commercial value.<sup>2</sup> The  $\text{TiO}_2/\text{PEO}$  photocatalyst partially changed the polyacetylene-like polymer into a PVA-like one and provided an improvement in the chloroform solubility. In addition, as shown in Table I, the PVA-like polymer had few carbon-carbon double-bond groups, and the PVA tacticity resonances appeared, as shown in Figure 7. The results show that the carbon-carbon double-bond group mostly converted to OH ones. The work of the  $\text{TiO}_2/\text{PEO}/\text{ML}$  photocatalyst was considerably different from that of the  $\text{TiO}_2/\text{PEO}$  one. The chloroform-soluble fraction contained the greatest methyl group content in all of the samples; this showed that the branching degree was the highest. In addition, the internal double-bond content was the highest as well. Figure 8 shows the  $^1\text{H}$ -NMR spectrum of the chloroform-soluble

fraction of the 24-h-photoirradiated PVC with  $\text{TiO}_2/\text{PEO}/\text{ML}$ . The apparent resonances assigned to the ML unit appeared around 1.6 and 3.6 ppm; this showed that there existed an ML radical structure in the sample. As shown in Scheme 2, the OH radical species was generated by the PEO photodegradation with  $\text{TiO}_2$ , and it attacked ML as well as PVC.<sup>7,8</sup> The ML radical species and polyene units were generated and then reacted each other. Although the OH radical species could react with the polyene as well, the ML radical species was preferentially added to it because of its good radical stability.<sup>7,8</sup> The addition of ML itself, having polyene units, led to a higher content of internal carbon-carbon double bonds, and additionally, autoxidation was facilitated to decrease the molecular weight<sup>7,8</sup> and simultaneously to crosslink. The decreases in the molecular weight and soluble fraction were due to the ML addition.

Because the UV-vis spectrum of the whole 24-h-photoirradiated PVC with  $\text{TiO}_2/\text{PEO}$  showed the maximum polyene length, the chloroform-insoluble part, having the polyene structure, must have existed more in it. To study the component in the chloroform insoluble part, the analytical pyrolysis (Py-GC/MS) was performed. Figure 9 shows the relative yields of HCl, benzene, and toluene in the fast pyrolysis of the chloroform-insoluble parts of the pristine PVC and 24-h-photoirradiated PVC samples with two kinds of photocatalyst. The relative amount of HCl decreased with increasing pyrolysis temperature, and this tendency was the same in all of the samples. Interestingly, the temperature tendency of the benzene relative amount in the sample with  $\text{TiO}_2/\text{PEO}$  was similar to that of the HCl one; it was considerably different from those of other samples. The other samples showed maximum values at 450°C. Benzene is a pyrolysate originated from a polyene unit,<sup>21–23</sup> and its amount certainly depended on the polyene unit content. In the sample with  $\text{TiO}_2/\text{PEO}$ , a strong negative correlation between the relative amount and pyrolysis temperature was seen. Because the sample contained more original polyene units, much benzene pyrolysate could be produced, even at 350°C. It seemed that the pyrolysis reaction became too fast at the higher temperature and mainly produced other

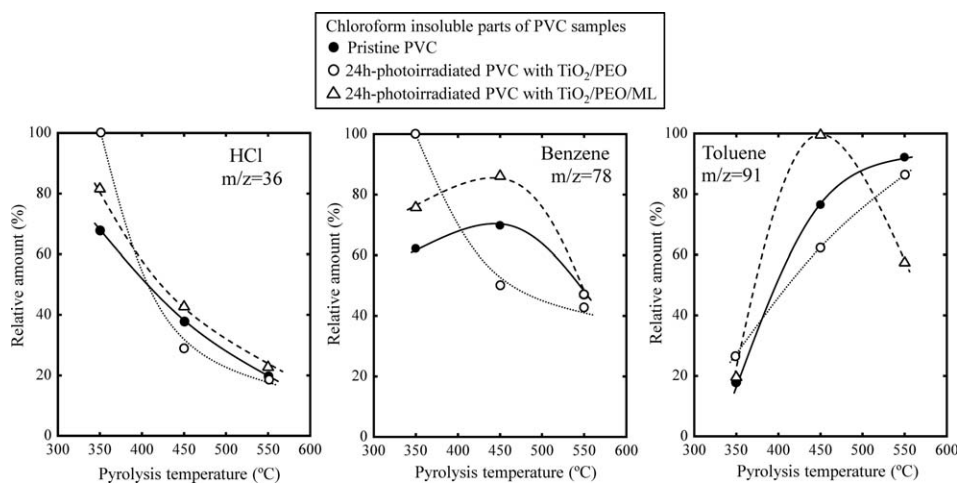


**Figure 9.** Relative yields of HCl, benzene, and toluene in the fast pyrolysis of the chloroform-insoluble parts of the pristine PVC and 24-h-photoirradiated PVC samples with two kinds of photocatalysts.

pyrolysates instead of benzene. Other samples with fewer polyene units required polyene production via dehydrochlorination. A temperature of 450°C was the optimum pyrolysis temperature for such a benzene pyrolysate production path. The different dependence of the pyrolysis temperature showed that more of the chloroform-insoluble part having the polyene structure existed in the whole 24-h-photoirradiated PVC with TiO<sub>2</sub>/PEO. The temperature tendency of the toluene relative amount was different from that of the HCl and benzene ones. Anthony<sup>22</sup> reported that toluene pyrolysate was formed via an intermediate composition of a crosslinked polyene structure.<sup>22</sup> The toluene production, therefore, was preferentially produced in the sample with a great amount of the crosslinked structure. As shown in Figure 9, the relative toluene amount of the sample with TiO<sub>2</sub>/PEO/ML showed the maximum value at 450°C, whereas those of other samples increased with the pyrolysis temperature. The difference was due to the ML-grafted structure in the sample with TiO<sub>2</sub>/PEO/ML. As shown in Scheme 2, the structure was a kind of crosslinked polyene one, and it certainly became a source of the formation of the toluene pyrolysate. A temperature of 450°C was the optimum pyrolysis temperature for the toluene pyrolysate production with the ML-grafted structure. The other samples required the production of a crosslinked polyene structure via a PVC pyrolysis reaction, which preferred a higher pyrolysis temperature. These results of the Py-GC/MS measurements show that the samples with TiO<sub>2</sub>/PEO and TiO<sub>2</sub>/PEO/ML contained such characteristic structures.

## CONCLUSIONS

PVC dehydrochlorination with paint photocatalysts was performed. The order of polyene length in the 24-h-photoirradiated PVC was as follows: With TiO<sub>2</sub>/PEO > With TiO<sub>2</sub>/PEO/ML ≥ Without photocatalyst > Pristine > With TiO<sub>2</sub>/PEO/MO. On the other hand, the order of the absorbance intensity was as follows: With TiO<sub>2</sub>/PEO/ML > TiO<sub>2</sub>/PEO = Without photocatalyst > Pristine > With TiO<sub>2</sub>/PEO/MO. These results show that the 24-h-photoirradiated PVC with TiO<sub>2</sub>/PEO had the structure with the longest polyene length and that with TiO<sub>2</sub>/PEO/ML had the greatest amount of the polyene structure. The order of the chloroform-soluble fraction amount was as follows: Pristine (18.6%) > With TiO<sub>2</sub>/PEO (13.2%) > With TiO<sub>2</sub>/PEO/ML (7.9%) ≥ Without photocatalyst (7.0%) > With TiO<sub>2</sub>/PEO/MO (3.3%). The chloroform-soluble fraction with TiO<sub>2</sub>/PEO provided the largest amount of the soluble fraction and contained the PVA structure instead of the polyene one. The GPC curve of the fraction shifted slightly to a lower molecular weight compared with that without the photocatalyst; this showed that slight polymer chain scission occurred. The <sup>1</sup>H-NMR and <sup>13</sup>C-NMR spectra showed that the content of the PVA unit was about 20%, and the PVA sequence was blocky. It was found that the OH substitution proceeded by a two-step reaction. On the other hand, the TiO<sub>2</sub>/PEO/ML made a difference to the PVC sample. This fraction contained the greatest methyl group content in all the samples; this showed that the branching degree was highest. In addition, the polyene content was highest as well. These highest contents were due to the existence of the grafted ML. The amount of the soluble fraction with TiO<sub>2</sub>/PEO/MO was lowest and was only 50% of that

with TiO<sub>2</sub>/PEO/ML. The MO grafting efficiency was considerably less because of the poor radical stability of MO, and the additive effect on the PVC solubilization was considerably less. The Py-GC/MS results suggest that there existed more polyene and graft units in the chloroform-insoluble fraction of the 24-h-photoirradiated PVC samples with TiO<sub>2</sub>/PEO and TiO<sub>2</sub>/PEO/ML.

## ACKNOWLEDGMENTS

This work was supported by the Japanese Ministry of the Environment through the Environment Research and Technology Development Fund (contract grant number 3K123020).

## REFERENCES

1. Nagai, Y.; Smith, R. L., Jr.; Inomata, H.; Arai, K. *J. Appl. Polym. Sci.* **2007**, *106*, 2007.
2. Kameda, T.; Fukuda, Y.; Grause, G.; Yoshioka, T. *Polym. Eng. Sci.* **2011**, *51*, 1108.
3. Shin, S.-M.; Yoshioka, T.; Okuwaki, A. *Polym. Degrad. Stab.* **1998**, *61*, 349.
4. Kamo, T.; Kondo, Y.; Kodera, Y.; Sato, Y.; Kushiya, S. *Polym. Degrad. Stab.* **2003**, *81*, 187.
5. Kameda, T.; Ono, M.; Grause, G.; Mizoguchi, T.; Yoshioka, T. *J. Polym. Res.* **2011**, *18*, 945.
6. Behnisch, J.; Zimmermann, H. *Int. J. Polym. Mater.* **1992**, *16*, 143.
7. Nakatani, H.; Miyazaki, K. *J. Appl. Polym. Sci.* **2013**, *129*, 3490.
8. Miyazaki, K.; Arai, T.; Nakatani, H. *J. Appl. Polym. Sci.*, to appear.
9. Kagiya, T.; Yokoyama, N.; Takemoto, K. *Bull. Inst. Chem. Res. Kyoto Univ.* **1976**, *54*, 15.
10. Ohtani, B.; Adzuma, S.; Miyadzu, H.; Nishimoto, S.; Kahiya, T. *Polym. Degrad. Stab.* **1989**, *23*, 271.
11. Turton, T. J.; White, J. R. *Polym. Degrad. Stab.* **2001**, *74*, 559.
12. Mina, M. F.; Seema, S.; Matin, R.; Rahaman, M. J.; Sarker, R. B.; Gafur, M. A.; Bhuiyan, M. A. H. *Polym. Degrad. Stab.* **2009**, *94*, 183.
13. Blakey, I.; George, G. A. *Polym. Degrad. Stab.* **2000**, *70*, 269.
14. Vijayalakshmi, S. P.; Madras, G. *J. Appl. Polym. Sci.* **2006**, *100*, 3997.
15. Miyazaki, K.; Nakatani, H. *Polym. Degrad. Stab.* **2009**, *94*, 2114.
16. Miyazaki, K.; Nakatani, H. *Polym. Degrad. Stab.* **2010**, *95*, 1557.
17. Broska, R.; Rychlý, J.; Csomorová, K. *Polym. Degrad. Stab.* **1999**, *63*, 231.
18. Eriksson, P.; Reiberger, T.; Stanberg, B. *Polym. Degrad. Stab.* **2002**, *78*, 183.
19. Rogstedt, M.; Hjertberg, T. *Macromolecules* **1993**, *26*, 60.
20. Winkler, D. E. *J. Polym. Sci.* **1959**, *35*, 3.
21. Blazsó, M.; Jakab, E. *J. Therm. Anal.* **1999**, *49*, 125.
22. Anthony, G. M. *Polym. Degrad. Stab.* **1999**, *64*, 353.
23. Montaudo, G.; Puglisi, C. *Polym. Degrad. Stab.* **1991**, *33*, 229.